Effects of Various Shot Peening Parameters on the Distribution of Residual Stresses and Microstructures of an 18CrNiMo7-6 Steel

F. Peng[1], J. Chuanhai[1], C. Xiaohu[2]

[1]School of Material Science and Engineering, Shanghai Jiaotong University
[2]Shanghai Carthing Machinery Co., Ltd.

Abstract:
Effects of shot peening (SP) parameters on the structure and residual stress of 18CrNiMo7-6 steel have been investigated using X-ray diffraction (XRD) analysis method. XRD pattern reveals that SP can induce the phase transformation from austenite to martensite. Results show that multi-step SP can significantly improve the compressive residual stress (CRS) and refine the domain size. After multi-step shot peeing with optimal intensities, CRS (martensite) at top surface attains 1,256 MPa, and maximum CRS of 1463 MPa is located at depth of 20 μm; maximum CRS and top-surface CRS (austenite) attains values of 1,039 MPa and 766 MPa, respectively. Obviously, domain sizes are decreased after SP.

Keywords: Shot peening; Residual stresses; Phase transformation; Microstructure

Introduction

18CrNiMo7-6 is a Chrome-Nickel-Moly carburising steel. It is widely used in many industrial components such as heavy-duty arbors, bushings, bearings, gears, shafts, sprockets, wear pins etc. due to its superior mechanical performance [1, 2]. However, mesh or angular carbide is often produced in carburizing process, and cracks are also produced in quenching or machining process. These cracks can reduce the fatigue strength and service life of 18CrNiMo7-6 steel components. Therefore, 18CrNiMo7-6 steel components often underwent surface treatment in order to increase its service life that depends mainly on the condition of the surface layer. SP is often used to improve the suface quality of the materials. It can create the beneficial CRS, thus inducing structure change and work hardening near the surface layer of a material [3-5]. The CRS produced in the surface layer of the parts that underwent the peening process can prevent or greatly delay the crack propagation, and thus improve fatigue behavior of material [6-8]. However, bombardments of the surface that was shot often lead to flaws or roughness increment, which may outweigh the beneficial effects of the compressive stresses induced by SP [9]. Previous work [7-11] has proved that SP can be beneficial to application of steel alloys if appropriate SP parameters are selected. Therefore, optimization of SP conditions is of great importance to maximize its beneficial effects. In this study, new multistep SP technologies with different parameters were studied in order to meet practical requirements. X-ray diffraction line profile analysis (XRDLPA) is a common non-destructive technique used to determine residual stresses in components in which crystalline planes are used as strain gauges [12]. Elastic strains induced by stress can cause spacing changes of atomic planes in these metallic crystal structures. These inter-planar atomic spacings can be directly measured via XRD method, thus total stresses on the metal can be calculated from elastic theory accordingly [13]. Besides, standard methods of XRDLPA are based on full width at half-maximum or integral breadths of profiles can be employed to calculate crystallite sizes [14]. In this study, XRDLPA is used to identify the structural changes and compressive stress distributions near peened surface layer of 18CrNiMo7-6 steel after SP.

Experimental

Materials

The studied material is case-hardened steel 18CrNiMo7-6 (EN 10084). Its chemical composition is: 0.17 C, 0.19 Si, 0.56 Mn, 1.52 Ni, 1.65 Cr, 0.32 Mo, 0.006 P, 0.0033 S, 0.028 Al, 0.02 Cu, 0.002 Sn and the balance Fe (weight %). All 18CrNiMo7-6 steel specimens were austenitized at 950 °C for 50 hours, subsequently heated at 860 °C for 2 hours and oil quenched, followed by tempering at 180 °C for 3 hours followed by air coolng.

Shot peening treatment

SP treatments were carried out via air blast machines (Carthing Machinery Company, Shanghai). SP intensities were measured by arc height of Almen specimen (A type). Different SP types (one SP, dual SP and triple SP) with different SP intensities (0.50 mmA, 0.30 mmA and 0.15 mmA) were carried out. Dual SP treatments were to execute 100% peening at 0.50 mmA followed by 100% at 0.30 mmA on the sample surface. Accordingly, triple SP is to go through 100% peening at 0.50 mmA followed by 100% at 0.30 mmA followed by 100% at 0.15 mmA. Cast steel balls with diameter of 0.6 mm and hardness of 610 HV and ceramic balls with diameter of 0.3 mm and hardness of 700 HV were used as shot media in the various SP techniques. Coverage of SP was 100% in each SP step.

Measurements

The surface layer was removed one by one via chemical etching method using saline solutions. At each depth, the residual stress and microstructure were evaluated. XRD patterns were measured by Rigaku Ultima IV diffractometer (Cu-Kα radiation) with a D/tex1D high-speed detector. Voltage, current, scanning velocity and step were 40 kV, 30mA, 2°/min and 0.02°, respectively. Residual stresses of samples were measured by X-ray stress analyzer (LXRD, Proto, Canada) with Ni filter (Cr Kα radiation for martensite and Mn Kα radiation for austenite). Voltage and current were 30 kV and 25 mA, respectively. Shifts of BCC $(211)_{\alpha}$ and FCC $(311)_{\gamma}$ peaks were detected in measurements and then residual stress was determined by $\sin^2\psi$ method [15, 16]. Peaks of $(211)_{\alpha}$ and $(311)_{\gamma}$ lattice plane were measured at high 2θ value of 156.4° and 152.8°, respectively.

Results and discussions

XRD patterns of top surface of 18CrNiMo7-6 steel before and after SP treatments are shown in Figure 1.

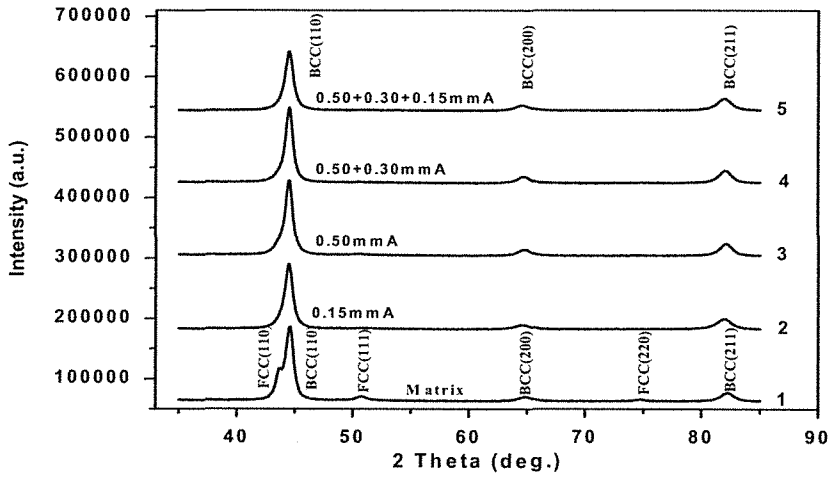

Figure 1: The surface X-ray diffraction patterns of 18CrNiMo7-6 steel before and after SP

The top surface of 18CrNiMo7-6 steel without SP possesses both austenite and martensite phase. Only martensite state was detected after SP, indicating that retained austenite had fully transformed to martensite during SP treatments. Depth distributions of residual stresses after SP with different parameters are shown in Figure 2 (martensite) and Figure 3 (austenite).

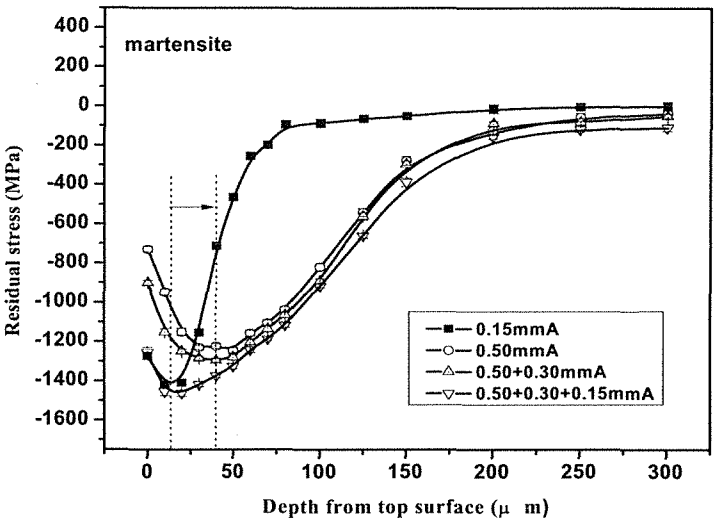

Fig. 2: Distributions of residual stresses (martensite) along depth after SP

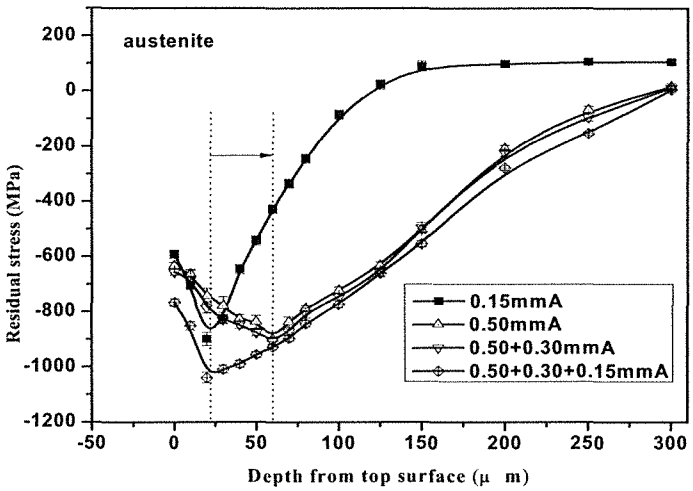

Fig. 3: Distributions of residual stresses (austenite) along depth after SP

In the range of testing, all samples after SP have obvious CRS. During SP, bombardment of hard balls with high velocity on the material surface will lead to repetitive plastic deformation of thin surface zones. Because of unequal plastic deformation between surface and internal layer of the material, SP induces a CRS at the surface and a compensation tensile residual stress inside the specimen away from the surface [17- 19]. Moreover, M. Kobayashi et al [20] think that CRS created by SP is considered to be a result of superposition of residual stress produced by surrounding shots. With increasing depths, CRS of all samples after SP increases firstly to the maximum, and then decrease gradually along the depth. Hertzian pressure distribution existing under the shot at the moment of impact predicts a maximum shear stress at the location below top surface, so the maximum of plastic deformation and residual stress occur below top surface [21]. Figure 2 illustrates that with the increase of SP intensities, CRS increases gradually. At the same depth, CRS of samples after triple SP are always greater than that of other samples. The maximum CRS and the top surface CRS of samples after triple SP attain values of 1463 MPa and 1276 MPa, respectively. The depth where MCRS is located attain 50 μm when SP intensity is 0.50 + 0.30 mmA. However, the depth where MCRS is located is only 20 μm when SP intensity is 0.50 + 0.30 + 0.15 mmA. Even so, at depth of 50 μm, CRS of the sample after triple SP is also higher than that of the sample after dual SP with

intensities of 0.50 + 0.30 mmA. Hertzian pressure effect is dominating in the processing of triple SP. The contact zone (a) between shot and material is narrow when triple SP with intensity of 0.50 + 0.30 + 0.15 mmA was executed owing to the higher hardness of the matrix after dual SP, the depth of MCRS ($Z_{\tau,max}$) for the sample after triple SP with intensity of 0.50 + 0.30 + 0.15 mmA is smaller owing to smaller *a* according to Eq. (1) [21].

$$Z_{\tau,max} = 0.47a \qquad (1)$$

where $Z_{\tau,max}$ is distinct distance below the surface, *a* is half width of contact zone.

Figure 3 shows the depth distributions of residual stress (austenite) after SP with different intensities. The changing rule of residual stress (austenite) as shown in Fig. 3 is very similar to that of residual stress (martensite) as discussed in Figure 2. With the increase of SP intensities, maximum CRS and top-surface CRS all increase, and CRS of the sample after SP with intensity of 0.50 + 0.30 + 0.15 mmA is always larger than that of any other samples at the same depth. Under the SP intensity of 0.50 + 0.30 + 0.15 mmA, MCRS and top surface CRS attain peak values of 1039 MPa and 766 MPa, respectively. From Figures 2 and 3, higher MCRS and top-surface CRS of martensite phase than that of austenite phase presumably results from peening-induced adiabatic heat production that is caused by extremely short impact durations of involving materials that are shot together with plastic deformation of various degrees according to different material hardnesses [22]. In soft materials, a sufficient rise in temperature may produce plastic compression of surface together with reduction of SP residual stresses. Therefore, in the present work, different CRS distributions and values between martensite phase and austenite phase under the same SP intensity demonstrate further because hardness of martensite phase is higher than that of austenite phase. Generally, deformation layer can induce CRS in both martensite state and austenite state after SP. CRS can effectively suppress crack initiation and propagation, and then improve fatigue properties [6-8]. Therefore, SP treatments can effectively improve service characters of 18CrNiMo7-6 steel; According to the discussions above, in terms of CRS, triple SP treatments with intensity of 0.50 + 0.30 + 0.15 mmA has the best effect.

In order to investigate microstructure variation, Cauchy breadths of (211) crystalline plane for martensite were calculated via normalized XRD patterns of all samples. Domain sizes of all samples were calculated via Voigt method [23, 24], and the result is shown in Figure 4.

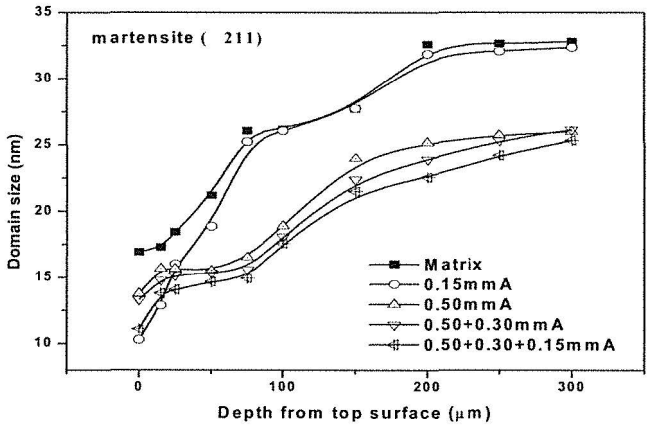

Fig.4 The depth distributions of domain size of the samples after SP

The domain sizes of all samples attain the minimum (around 15 nm or lower) at the top surface, and then increase gradually along depths. At all depths, domain sizes after triple SP attain the minimum value. This is because the following SP treatments after the first SP or dual SP can still further add plastic deformation and further refine domain sizes. The refined domain can improve mechanical properties of materials. Therefore, SP treatments, especially with reasonable SP conditions, can be seen as an effective method to improve mechanical properties of materials.

Conclusion

The effect of multistep SP on the microstructure and CRS distributions of 18CrNiMo7-6 steel were studied. Results show that triple SP is an effective way to optimize CRS and microstructure of 18CrNiMo7-6 steel. The triple SP with intensity of 0.50 + 0.30 + 0.15 mmA has the best effect on the properties of 18CrNiMo7-6 steel. For martensite, CRS attains 1,256 MPa at top surface, and MCRS attains 1,463 MPa at depth of 20 μm. For austenite, MCRS and top-surface CRS are 1,039 MPa and 766 MPa, respectively. Domain sizes of the sample after triple SP decrease obviously compared with other samples.

References

[1] J. X. Liu, Z. J. He, L. H. Wang, G. P. Feng, Z. J. Zhang, et al, Adv Mater Res 2011; 194-196: 228-31.
[2] J. Krawczyk, B. Pawlowski, P. Bala, Metall. Foundry Eng. 2009; 35: 45.
[3] S. P. Wang, Y. J. Li, M. Yao, R. Z. Wang, J Mater Process Tech 1998; 73: 64-73.
[4] R. Shivpuri, , X. M. Cheng, Y. N. Mao, Mater Design 2009; 30: 3112-20.
[5] Peng Fu, K. Zhan, C. H. Jiang, Mater Design 2013; 51: 309-14.
[6] W. Luan, C. Jiang, V. Ji, Y. Chen, H. Wang, Mater Sci Eng A 2008; 497: 374-7.
[7] S. Bagherifard, R. Ghelichi, M. Guagliano, Surf Coat Tech 2010; 204: 4081-90.
[8] M. A. S. Torres, H. J. C. Voorwald, Int J Fatigue 2002; 24: 877-86.
[9] J. Lindemann, C. Buque, F. Appel, Acta Mater 2006; 54: 1155-64.
[10] N. Barry, S.V. Hainsworth, M.E. Mater Sci Eng A 2009; 507: 50-7.
[11] S Tekeli, Mater Lett 2002; 57: 604-608.
[12] M. Gelfi, E. Bontempi, R. Roberti, L. E. Depero, Acta Mater 2004; 52: 583-9.
[13] N. S. Rossini, M. Dassisti, K. Y. Benyounis, A. G. Olabi, Mater Design 2012; 35: 572-88.
[14] J. Gubicza, M. Kassem, G. Ribárik, T. Ungár, Mater Sci Eng A 2004; 372: 115-22.
[15] E. Macherauch, Exp mech 1966; 6: 140-53.
[16] Jonathan D. Almer, Robert A. Winholtz, Springer handbook of experimental solid mechanics, 2008: 801-20.
[17] P. Fu, K. Zhan, C. H. Jiang, Mater. Design 2013; 51: 309.
[18] K. Zhan, C. H. Jiang, X. Y. Wu, V. Ji, Mater Trans 2012; 53: 1002-6.
[19] K. Dalaei, B. Karlsson, L.-E. Svensson, Mater Sci Eng A 2011; 528: 1008-15.
[20] M. Kobayashi, T. Matsui, Y. Murakamit, Int. J. Fatigure, 1998; 20: 35-357.
[21] H. Wohlfahrt, ICSP-2, Chicago,1984: 316–331.
[22] O. Vöhringer, ICSP3, Verlag, 1987: 185–204.
[23] T. Ungár, A. Borbély, Appl. Phys. Lett. 1996; 69: 3173.
[24] T. Ungár, J. Gubicza, G. Ribárik, A. Borbély, J. Appl. Cryst. 2001; 34: 298.